Determination of the friction coefficient of coal particles by discrete element simulation and experimentation

Jinrong CHAI (xiaozheng3340@yeah.net)
China University of Mining and Technology(Beijing)
Shifeng WANG
China University of Mining and Technology(Beijing)
Zihao ZHOU
China University of Mining and Technology(Beijing)
Guohua LI
China University of Mining and Technology(Beijing)
Xunan LIU
Liaoning Technical University

Research Article

Keywords: coal particle, friction coefficient, discrete element simulation, simulation model

Posted Date: December 15th, 2020

DOI: https://doi.org/10.21203/rs.3.rs-122784/v1

Determination of the friction coefficient of coal particles by discrete element simulation and experimentation

Chai Jinrong[1], Wang Shifeng[1], Zhou Zihao[1], Li Guohua[1], Liu Xunan[2]

1.School of Mechanical Electronic and Information Engineering, China University of Mining and Technology(Beijing), Beijing 100083, China;

2.College of Mechanical Engineering, Liaoning Technical University, Fuxin, 123000, China）

these authors contributed equally to this work

ABSTRACT

The friction coefficient of coal is the main factor influencing the results of discrete element simulation. In this study, the friction coefficient of coal was determined using a self-made testing instrument for measuring the static friction coefficient and an automatic cylinder lifting device on the basis of discrete element simulation, image processing, and orthogonal testing. The correlations between the angle of repose of coal particles, the rolling friction coefficient between coal particles, and the rolling friction coefficient between the coal particles and stainless steel were evaluated by linear regression analysis. Results indicated that the dependent variable (angle of repose of coal particles) was linearly correlated to the two independent variables (rolling friction factor between the coal particles, as well as the rolling friction factor between the coal and the stainless steel). The angle of repose of the coal particles was largely affected by the rolling friction coefficient between the coal particles but not by the rolling friction coefficient between the coal particle and stainless steel. Moreover, the static friction coefficient between the coal particles was 0.53, and that between the coal particle and the stainless steel was 0.38. The rolling friction coefficient between the coal particles was 0.048, and that between the coal particles and the stainless steel was 0.03. These friction coefficients were used to simulate the bottomless cylinder test of the coal particles. The angle of repose in the simulation test was 30.77°, whereas that in the real test was 31.47°; the relative error was 2.22%. Therefore, no significant difference in the results was indicated between the simulation test and the real test, verifying the effectiveness of the method used to determine friction coefficients. The aforementioned technique can be applied to determine the friction coefficient of lump coal particles.

Key words: coal particle; friction coefficient; discrete element simulation; simulation model

Introduction

Discrete element simulation has been widely used in the coal mining industry, particularly in coal mining and conveying[1–8]. The physical characteristic parameters (Poisson's ratio, shear modulus, density) and contact parameters (collision recovery coefficient, static friction factor, and rolling friction factor) of discrete element simulation materials significantly influence the simulation test results[9–10]. The physical properties of the material can be measured by a triaxial shear test, a tensile pressure test, and a uniaxial compression test[11–14]. Material density can be determined using the drainage method. However, the contact parameters of materials are difficult to determine directly through experiments, requiring calibration with discrete element simulation software. Wen Xiangyu et al. [15] fitted the relationship between the contact parameters of granular fertilizers and the overall characteristics of the material through a simulation test. They also derived the contact parameters of granular fertilizers from actual test results. Yuan Quanchun et al. [16] established a regression

model through a simulation test and combined the result with that of the physical test to identify the optimal method for determining the simulation model parameters of organic fertilizers. Li Tiejun et al. [13] conducted a Box–Behnken simulation test on the friction factor of 6–8 mm coal particles; moreover, they solved the regression model with the actual stacking angle as the response value, identifying the optimal combination of the contact parameters of coal particles.

Currently, studies on methods for determining the contact parameters of granular materials mainly focus on granular materials related to agriculture [17–18]; meanwhile, few studies have been reported on the contact parameters of coal particles. Various coal particles have large granularity spans and different contact parameters for different coal particles. The application of discrete element simulation in the mining industry necessitates the study of the contact parameters of coal particles. Based on previous studies, the current study uses a self-made static friction factor tester and an automatic cylinder lifting test device. This study also combines discrete element simulation, image processing technology, orthogonal testing, and regression analysis to examine the discrete element simulation friction factor of lump-coal with particle sizes of 24–26 mm.

1 Materials and Methods

1.1 Basic parameters of the test materials

The coal particles used in the experiment are anthracite from Shanxi Province. Anthracite is a hard, dense, and high-gloss variety of coal mine, with grain sizes ranging from 24 mm to 26 mm. The material in contact with the coal particles is stainless steel. The Poisson ratio, shear modulus, density, and recovery coefficient of the selected materials were determined by referring to relevant literatures[12,18]. The basic parameters of the materials are listed in Tab. 1.

Table 1 Basic material parameters[12, 18]

Materials	Parameters	Value
Coal	Poisson's ratio	0.3
	Shear modulus/Pa	2×10^8
	Density/(kg/m^3)	1500
	Coal–coal restitution coefficient	0.64
	Coal–stainless steel restitution coefficient	0.65
Stainless steel	Poisson's ratio	0.29
	Shear modulus/Pa	8×10^8
	Density/(kg/m^3)	7800

1.2 Experimental method

1.2.1 Static friction factor calibration testing

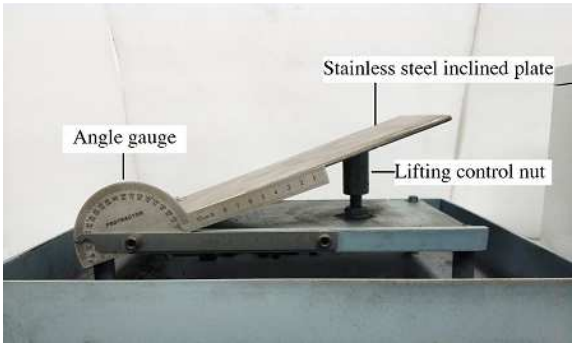

Figure 1 Test instrument of the static friction coefficient

The static friction factor test was conducted on a self-made tester (Fig. 1) . The static friction factor between the coal and the stainless steel plate was measured as follows: The coal particles were placed on a stainless steel inclined plate, which was then tilted slowly. The inclined plate angle when the coal particles

began to slide was recorded; this step was repeated 3 times, and the average of the 3 test results was calculated. The coal and the coal static friction factor were determined as follows: The large flat coal was selected and then fixed on the stainless steel plate by using glue. The coal particles were then placed on the large flat coal. The stainless steel inclined plate was slowly tilted. The angle when the coal particles started to slide on the large flat coal was recorded; this step was repeated 3 times, and the average of the 3 test results was determined. The static friction factor, static μ, was calculated using Eq.(1).

$$\mu = \tan(\alpha) \tag{1}$$

1.2.2 Rolling friction factor calibration testing

An orthogonal simulation experiment on coal particle stacking was conducted using the discrete element simulation software EDEM. With the real stacking angle as a reference, the orthogonal simulation results were analyzed. Regression analysis of the orthogonal simulation results was performed to establish the relationship between the rolling friction factor and the angle of repose. The rolling friction factor of the coal particles was solved.

1) Discrete element simulation model of coal particles

The choice of the coal particle model influences the simulation results to a certain extent. Xia Rui [19] et al. established six coal particle models to evaluate the effects of the models on the accuracy of the simulation; the research results showed that the 10-ball particle model exhibited the highest accuracy. The 10-ball coal particle model is presented in Fig. 2.

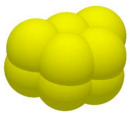

Figure 2 Model of the coal particles

2）Contact model of discrete element simulation

In the actual test, the dry coal particles was used as the test material, and the surfaces of the coal particles almost exhibited no adhesion. Therefore, the Hertz–Mindlin (no-slip) contact model, which exhibits rapid calculation and high precision, was adopted as the contact model between coal particles and between the coal particles and stainless steel in the simulation. The normal component in the model was calculated based on the Hertz theory of contact mechanics, and the tangential component was calculated based on the research results of Mindlin and Deresiewicz. Both normal force and tangential force have damping components, and the damping coefficient is related to the particle recovery coefficient[19]. Tangential friction follows Coulomb's law of friction[20], and rolling friction can be explained by the directional constant torque of the contact surface[21]. The specific formula is as follows[22] :

The normal force between particles (F_n) can be determined using Eq. (2):

$$F_n = \frac{4}{3} E^* (R^*)^{1/2} (R_1 + R_2 - |r_1 - r_2|)^{3/2} \tag{2}$$

where R^* is the equivalent particle radius of two spherical particles in elastic contact, which can be derived from Eq. (3); E^* is the equivalent elastic modulus, which can be determined from Eq. (4); r_1, r_2 are the position vectors from the center of the two particles.

$$\frac{1}{R^*} = \frac{1}{R_1} + \frac{1}{R_2} \tag{3}$$

where R_1 and R_2 denote the radii of the two particles in contact.

$$\frac{1}{E^*}=\frac{1-\nu_1^2}{E_1}+\frac{1-\nu_2^2}{E_2} \tag{4}$$

where E_1, ν_1, E_2 and ν_2 are the elastic moduli and Poisson's ratios, respectively, of the two particles.

The normal damping force F_n^d can be calculated using the following equation:

$$F_n^d=-2\sqrt{\frac{5}{6}}\frac{\ln e}{\sqrt{\ln^2 e+\pi^2}}\sqrt{S_n m^*}v_n^{rel} \tag{5}$$

where e is the recovery coefficient; S_n is the normal stiffness, which can be determined using Eq. (6); v_t^{rel} is the normal component value of the relative velocity.

$$S_n=2E^*\sqrt{R^*(R_1+R_2-|r_1-r_2|)} \tag{6}$$

The tangential force F_t between the particles can be obtained from the following formula:

$$F_t=-8G^*\sqrt{R^*(R_1+R_2-|r_1-r_2|)\delta} \tag{7}$$

where G^* is the equivalent shear modulus, which can be calculated from Eq. (8); δ is the tangential overlap quantity.

$$G^*=\frac{2-\nu_1^2}{G_1}+\frac{2-\nu_2^2}{G_2} \tag{8}$$

where G_1, G_2 are the shear moduli of the two particles.

The tangential damping force F_t^d between the particles can be calculated using the following formula.

$$F_t^d=-2\sqrt{\frac{5}{6}}\frac{\ln e}{\sqrt{\ln^2 e+\pi^2}}\sqrt{S_n m^*}v_t^{rel} \tag{9}$$

where v_t^{rel} is the tangential component value of the relative velocity.

The tangential force $\mu_s F_n$ is also related to the friction force μ_s and is the static friction factor.

The moment of the contact surface is related to the rolling friction factor, as shown in Eq. (10).

$$T_i=-\mu_r F_n R_i \omega_i \tag{10}$$

where μ_s is the rolling friction factor between particles; R_i is the distance between the center of mass and the contact point; ω_i is the unit angular velocity vector of the object at the point of contact.

By using this contact model, the force on coal particles can be decomposed into two directions: the normal direction and the tangential direction of the contact point. The force in each direction can be simplified into the force exerted by the spring and the damping force. The tangential force is affected not only by the elastic force and the damping force but by the friction force as well. The contact model measures the resultant force of forces in the normal and tangential directions to determine the spatial force of coal particles in contact collision. It also calculates the position of coal particles at each time step by iteration.

3) Simulation model of the bottomless cylinder tester

The size of the bottomless cylinder should be determined based on the predicted particle size. The bottomless cylinder should have a diameter larger than 4–5 times the maximum particle size and a height-to-diameter ratio of 3:1[23]. Given that the predicted coal particle size was 24–26 mm, the bottomless barrel measured 130 mm in diameter and 390 mm in height. In the EDEM software, the cylinder modeling tool in Geometry was used to establish the bottomless cylinder discrete element model with determined parameters and to set the stainless steel as the material. With the polygon modeling tool in Geometry, a 600 mm × 600 mm plane was established, and stainless steel was set as the material. The plane of the stainless steel plate coincided with the bottom plane of the bottomless cylinder.

4) Simulation of the bottomless cylinder test

After the geometry of the bottomless cylinder and stainless steel plate was generated, the polygon modeling tool in Geometry was used to establish a plane measuring 90 mm × 90 mm on the upper end of the bottomless cylinder, and the plane was set as a virtual plane. A particle factory was established on the virtual plane. Coal particles were produced by dynamic quantitative particle generation, and the simulated coal particles were filled with a bottomless cylinder. After the particles were stabilized in the bottomless cylinder, the bottomless cylinder was set to move in a positive direction perpendicular to the plane of the stainless steel plate at the speed of 0.01 m/s. The coal particles gradually flowed out, eventually forming a heap of stable cone particles on the stainless steel plate. The simulation process is illustrated in Fig. 3.

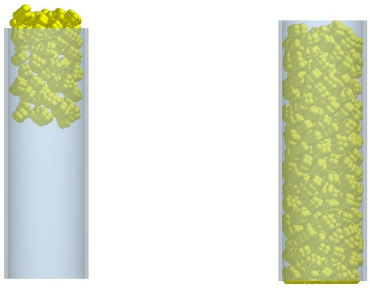

(a) Coal particles being packed into the bottomless cylinder (b) Bottomless cylinder filled with coal particles

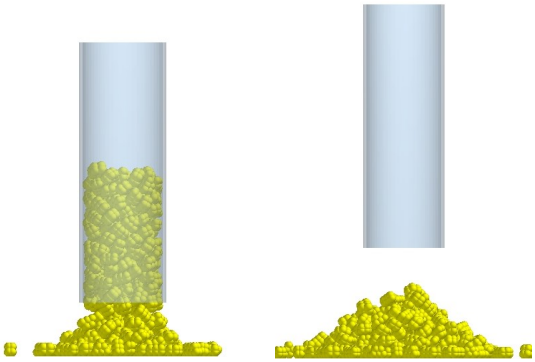

(c) Coal particles flowing out (d) Formation of a pile of coal particles

Figure 3 Simulation of the bottomless cylinder test

5) Measurement of the angle of repose

The stacking contour of the coal particles was formed by the particles and was not a straight line. If the angle of repose of the coal particles was measured using a screen protractor, errors would be generated. To more accurately measure the angle of repose of the coal particles, the measurement method described in the literature[15, 24] was adopted in the current study, and the specific method is illustrated in Fig. 4. The original image was show in Fig. 4a. First, Matlab was used to process the image and consequently produce the binary image (Fig. 4b). Second, the boundary contour of the binary graph was extracted (Fig. 4c). Third, the boundary contour of the binary graph was scanned, the coordinates of the white points were recorded, the boundary contour was fitted linearly by using the least-squares method, and the fitting line was drawn with the red line (Fig. 4d). The slope K of the fitting line was read in the Matlab software working area, and the inclination of the edge contour of the particle heap was be established using Formula 11. In each simulation, the particle heap morphology diagram was intercepted in the positive X and positive Z directions. The angle of repose was considered as the average of the angles of repose in the positive X and positive Z directions. Each simulation experiment was repeated 3 times, the average of the 3 test results was determined.

$$\theta = \frac{\arctan|k| \times 180}{\pi} \tag{11}$$

5）Orthogonal experimental design

The orthogonal test table of two factors and three levels was designed, and the orthogonal simulation test was performed. Regression analysis was also conducted to determine the relative relationship between the dependent variable (angle of repose of coal particles) and two independent variables (the rolling friction factor between coal paritcles, as well as the rolling friction factor between coal and stainless steel). The orthogonal test table of two factors and three levels is shown in Tab. 2.

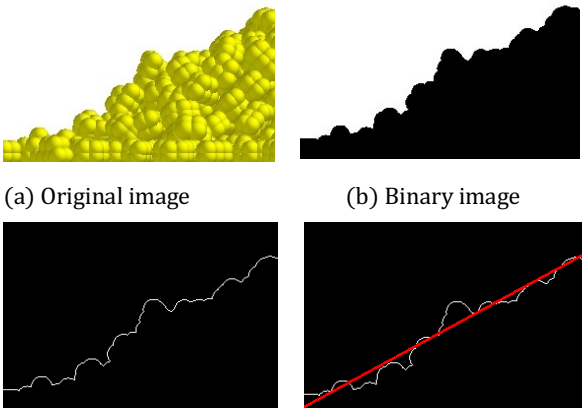

(a) Original image (b) Binary image

(c) Boundary contour image (d) Contour fitting image

Figure 4 Image processing of the angle of repose measurement

6) Regression analysis

To analyze the effects of the factors A and B on the angle of repose, regression analysis of the aforementioned orthogonal test data was conducted. The angle of repose was considered as the dependent variable, whereas the rolling friction factor between the coal particles (A) and the rolling friction factor between the coal and stainless steel (B) were regarded as the independent variables.

Table 2 Orthogonal test table

No.	A (Rolling friction factor between coal and coal)	B (Rolling friction factor between coal and stainless steel)
1	1 (0.01)	1 (0.01)
2	1	2 (0.03)
3	1	3 (0.05)
4	2 (0.03)	1
5	2	2
6	2	3
7	3 (0.05)	1
8	3	2
9	3	3

2 Results and analysis

2.1 Static friction factor

The inclination angles of the inclined plates in the three static friction factor tests of coal particles to coal particles were 27.5°, 28.5°, and 28°, with 28° as the average value. By substituting the average value into Formula 1, the static friction factor between the coal particles was calculated as 0.53. The inclined plates of the

static friction factor tests between the coal particles and stainless steel, performed three times, were 21°, 21°, and 20.5°, respectively. The average value was 20.83°, which was then substituted into Formula 1 to calculate the static friction factor between the coal particles and stainless steel (0.38).

2.2 Rolling friction factor

2.2.1 Analysis of the orthogonal test results

The orthogonal test results are listed in Table 3. With the measured angle of repose as the reference (the measured angle of repose was tested in the third part), the orthogonal test data were analyzed. The optimal horizontal combination was determined as A3B2—that is, when the rolling friction factor between the coal particles was 0.05, the rolling friction factor between the coal and stainless steel was 0.03, yielding the simulation result closest to the actual value.

Table 3 Analysis of orthogonal test results

NO.	A (rolling friction factor between coal particles)	B (rolling friction factor between coal particles and stainless steel)	K (slope of the fitted curve)	Θ (angle of repose)	Error (%)
1	1 (0.01)	1 (0.01)	-0.4986	26.51°	15.76%
2	1	2 (0.03)	-0.5146	27.24°	13.44%
3	1	3 (0.05)	-0.5147	27.23°	13.47%
4	2 (0.03)	1	-0.5594	29.24°	7.09%
5	2	2	-0.5770	29.53°	6.16%
6	2	3	-0.5531	28.96°	7.98%
7	3 (0.05)	1	-0.5966	29.86°	5.12%
8	3	2	-0.6350	32.43°	3.05%
9	3	3	-0.6494	33.03°	5%
K1	42.67	27.97			
K2	21.23	22.65			
K3	13.17	26.45			
k1	14.22	9.32			
k2	7.08	7.55			
k3	4.39	8.82			
R	9.83	1.77			
The optimal level	A3	B2			

2.2.2 Regression analysis results

Linear regression analysis of the test data in Tab. 3 was conducted to establish the prediction model of the angle of repose of the bottomless cylinder test (Eq. (12)).

$$\theta = 24.86 + 118.75A + 30.08B \tag{12}$$

The analysis of the regression model indicated that R^2 of the prediction model of the angle of repose was 0.90, and the prediction model has a satisfactory goodness of fit. The significance of the prediction model was less than 0.05, indicating a significant linear correlation between the dependent variable (repose angle) and independent variables (the rolling friction factor between coal particles and the rolling friction factor between the coal and stainless steel). The significance of the prediction model constant and the rolling friction factor between the coal particles was less than 0.001, indicating that the constant of the model and the rolling friction factor between the coal particles are extremely significant. The significance of the rolling friction factor between the coal and stainless steel was 0.118>0.05, indicating no significance in the rolling friction factor

between the coal and stainless steel.

The rolling friction factor of the coal to stainless steel exerted no significant influence on the angle of repose. Thus, the rolling friction factor between the coal and stainless steel could choose the optimal value, which determined by the orthogonal test, i.e. 0.03. The value of the rolling friction factor between the coal and stainless steel was substituted into Formula (12) of the prediction model, and the calibration value of the rolling friction factor between the coal and stainless steel was calculated as 0.048.

3 Validation test

The test was conducted on a self-developed automatic cylinder lifting device. The testing machine had a lead screw slider structure, which was driven by a servo motor for rotating the lead screw. The slider moved up and down as the lead screw rotated, and a bottomless cylinder was connected to the slider, rising at a constant speed with the slider. The machine was equipped with a servo control system to control the lifting speed of the bottomless cylinder and reduce the test error caused by factors such as the shaking, eccentricity, and unstable speed of the bottomless cylinder. The automatic cylinder lifting device is shown in Figure 5. The bottomless cylinder has a lifting speed of 0.01 m/s, which was consistent with the condition for the simulation test of the bottomless cylinder. The coal particles used in the test were anthracite from Shanxi Province, and the particle size ranged from 24 mm to 26 mm. The experiment was repeated three times, and the average value was taken.

The static friction factor between the coal particles, the rolling friction factor between the coal particles and stainless steel plate, and the rolling friction factor between the coal particles and stainless steel plate were input into the bottomless cylinder system for the accumulation simulation test. The experiment was repeated three times, and the average value was taken. Figure 6 presents the diagram of the comparison between the real and simulation tests. The two exhibited similar stacking morphologies; however, the slope surface of the real test was smoother than that of the simulation test because the dispersion of the coal particle size in the simulation process and that in the real test varied to a certain extent.

The angles of repose for the three repeated tests in the real experiment were 31.72°, 33.26°, and 29.37°, respectively, with a mean value of 31.47° and a standard deviation of 1.6°. The angles of repose of the coal blocks obtained from the real experiment were 31.47°±1.6°. The angles of repose for the three replicates of the simulation test were 31.22°, 30.77°, and 30.31°, respectively, with a mean value of 30.77°and a standard deviation of 0.37°. The angles of repose of the coal obtained from the simulation test were 30.77°±0.37°. The angle of repose error obtained from the simulation test was 2.22%. The friction factor of the coal particles can be determined using the discrete element method combined with image processing, orthogonal testing, and linear regression.

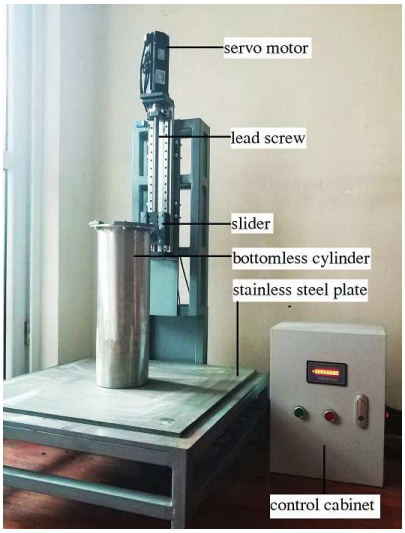

Figure 5 Automatic cylinder testing machine

(a) Actual test

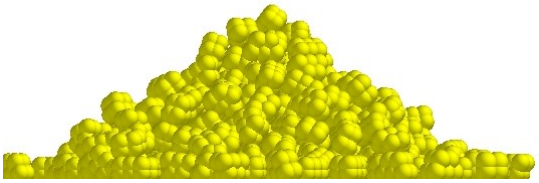

(b) Simulated test

Figure 6 Comparison between actual and simulated tests of coal particle accumulation

4 Conclusion

(1) The static friction factor between the coal particles was 0.53, and that between the coal and stainless steel was 0.38, as determined using the slope test.

(2) The influence of the rolling friction factor between the coal particles and that between the coal and the stainless steel plate on the angle of repose for the coal particles was evaluated using the orthogonal simulation experiment. With the real stacking angle as a reference, orthogonal test data were analyzed. The analysis results indicated that the smallest error between the simulation value and the real value was generated when the rolling friction factor between the coal particles was 0.05 and the rolling friction factor between the coal and the stainless steel plate was 0.03.

(3) Linear regression analysis of the orthogonal experimental data was conducted. The results showed that a linear correlation was present between the dependent variable (angle of repose of coal particles) and two independent variables (the rolling friction factor between the coal particles, as well as that between the coal and the stainless steel). The angle of repose of the coal particles was largely affected by the rolling friction coefficient between coal particles but not by the rolling friction coefficient between the coal particle and the stainless steel. The rolling friction factor between the coal particles and the stainless steel plate was considered as the optimal value of orthogonal analysis (0.03); when substituted into the regression equation, the rolling friction factor between the coal particles was calculated as 0.048.

(4) The aforementioned coal particle friction factor was input into the discrete element simulation model for the simulation test of the angle of repose. The angle of repose in the simulation was 30.77°, whereas that in the actual test was 31.47°; the relative error was 2.22%.

This method can be used to determine the friction factor of dry anthracite particles. The influence of other factors—such as coal type, degree of coal irregularity, and coal particle size distribution—on the accumulation characteristics has yet to be further studied to continuously improve the accuracy of this method and expand its scope of application.

Reference

1. Gao, K. D., Wang, L. P., Du, C. L., Li, J. N., Dong, J. H.. Research on the effect of dip angle in mining direction on drum loading performance: a discrete element method. *The International Journal of Advanced Manufacturing Technology,* 89: 2323-2334 (2017).

2. Mao, J., Liu, X. Y., Chen, H. Y., Song Q. S.. Simulation of shearer drum cutting performance based on EDEM. *Journal of China Coal Society,* 42(4):1069-1077(2017).
3. Li, X. F., Wang, S. B., Ge, S. R., Malekian, Reza，Li, Z. X.，et al. A study on drum cutting properties with full-scale experiments and numerical simulations. Mea*surement,* 114: 25-36(2018).
4. Zhao, L. J., Jin, X., Zhao Y. D., Wang, B.. Discrete element simulation analysis on the wear characteristics of drum in coal seam with gangue. *Journal of China Coal Society,* 45(9) :3341-3350 (2020).
5. Wang, X. W., Li, B., Yang, Z. J.. Analysis of the Bulk Coal Transport State of a Scraper Conveyor Using the Discrete Element Method. *Strojniški vestnik-Journal of Mechanical Engineering,* 64(1): 37-46(2018).
6. Gong, Z. Q., Wang, D. C., Wang, G. H., Wu, H. J., Gu, X. W.. Simulation analysis and design of vertical screw silage-conveyor based on EDEM. ASABE Annual International Meeting (2016).
7. Barrios, Gabriel, K.P., de Carvalho, Rodrigo M., Kwade, Arno, Tavares, Luís Marcelo, Tavares, Luís Marcelo. Contact parameter estimation for DEM simulation of iron ore pellet handling. *Powder Technology,* 248（2）: 84-93(2013).
8. Wei, X.. Research on the wear of scraper conveyor chute based on DEM *(*M.S. *Thesis)*. Taiyuan: Taiyuan University of Technology, China (2019).
9. Martina, C. L., Bouvarda, D., Shimad, S.. Study of particle rearrangement during powder compaction by the discrete element method. *Journal of the Mechanics and Physics of Solids,* 51(4) : 667-693 (2003).
10. Cleary, P. W.. Predicting charge motion, power draw, segregation and wear in ball mills using discrete element methods. *Minerals Engineering,* 11(11) : 1061-1080(1998).
11. Zhang R., Han D., Ji Q., He, Y., Li, J.. Calibration methods of sandy soil parameters in simulation of discrete element method. *Transactions of the Chinese Society for Agricultural Machinery*，48(3)：49-56(2017).
12. Shi L. R., Sun, W., Zhao, W. Y., Yang, X. P., Feng B.. Parameter determination and validation of discrete element model of seed potato mechanical seeding. *Transactions of the CSAE*, 34(6) : 35-42(2018).
13. Li, T. J., Wang, X. W., Li, B., Li, J. L., Yang, Z. J.. Optimization method for coal particle model parameters based on discrete element method. *CHINA Powder Science and Technolgy*，24(5) : 6-12(2018).
14. Wang, J. F., Ju, J.Y., Yin, D. Q..Test and analysis of elastic modulus of urea particle．*Journal of Anhui agriculture science*,42(33) : 11626-11628 (2014).
15. Wen, X. Y., Yuan, H. F., Wang, G., Jia, H. L.. Calibration Method of Friction Coefficient of Granular Fertilizer by Discrete Element Simulation. *Transactions of the Chinese Society of Agricultural Machinery*, 51（2）：115-122,142(2020).
16. Yuan, Q. C., Xu, L. M., Xing, J. J., Duan, Zh. Zh., Ma, Sh., et al. Parameter calibration of discrete element model of organic fertilizer particles for mechanical fertilization. *Transactions of the CSAE*，34(18) : 21-7 (2018).
17. Feng, B., Sun, W., Shi, L. R., Sun, B. G., Zhang, T., et al. Determination of restitution coefficient of potato tubers collision in harvest and analysis of its influence factors. *Transactions of the Chinese Society of Agricultural Engineering*，33（13）：50-57(2017).
18. Lou, S., Yuan, Q. X., GOUDA, S., Yang, L. Y., et al. Parameters Calibration of Vermicomposting Nursery Substrate with Discrete Element Method Based on JKR Contact Model. *Transactions of the Chinese Society for Agricultural Machinery*, 49(04)：343-350 (2018).
19. Tsuji, Y., Tanaka, T., Ishida, T.. Lagrangian numerical simulation of plug flow of cohesionless particles in a horizontal pipe. *Powder Technology*, 71（3）：239-250 (1992).
20. Sakaguchi H., Ozaki, E., Igarashi, T.. Plugging of the Flow of Granular Materials during the Discharge from a Silo. *International Journal of Modern Physics B*. 7(9):1949-1963(1993).
21. Cundall, P. A., Strack, O. D. L.. A discrete numerical model for granular assemblies. *Géotechnique*, 29(1):47-65 (1979).
22. Wang G. Q., Hao, W. J., Wang, J. X.. Discrete Element method and its practice on EDEM. Northwest Polytechnic University Press，China(2010).
23. Wu A. X, Sun, Y. Zh., Liu, X. P.. Theory and application of granular dynamics. Metallurgy Press, China(2002).
24. Jia, F. G., Han, Y. L., Liu, Y., Cao, Y., Wang, H.. Simulation prediction method of repose angle for rice particle materials. *Transactions of the Chinese Society of Agricultural Engineering*，30（11）:254-260.(2014)

Acknowledgments

This study was supported by the National Key Researcher and Development Plan during the 13th Five-Year Plan of China (2017YFB0305105).

Author contributions

The contributions of the authors are as follows: J. R. C.: proposed the problem and was responsible of the discussion and writing of the manuscript. S.F.W.: was responsible of experiment. Z. H. Z.: was responsible of

simulation. G. H. L. and X. N. L.: were responsible of writing of the manuscript.

Competing interests

The authors declare no competing interests

Additional information

Correspondence and requests for materials should be addressed to J. R. C..

Reprints and permissions information is available at www.nature.com/reprints.

Publisher’ s note Springer Nature remains neutral with regard to jurisdictional claims in published maps and institutional afliations.

Corresponding author

Correspondence to Jinrong Chai. The email address of corresponding author is xiaozheng3340@yeah.net.

Figures

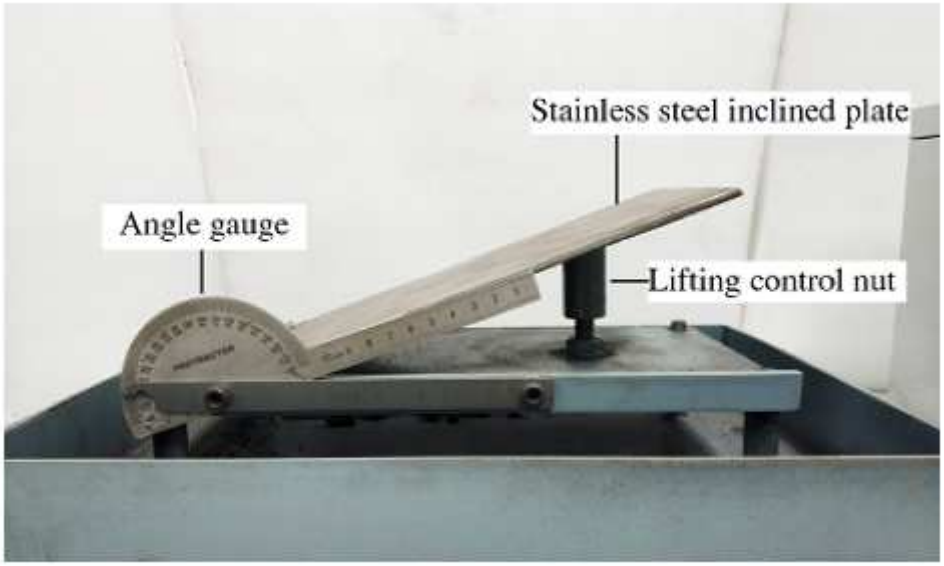

Figure 1

Test instrument of the static friction coefficient

Figure 2

Model of the coal particles

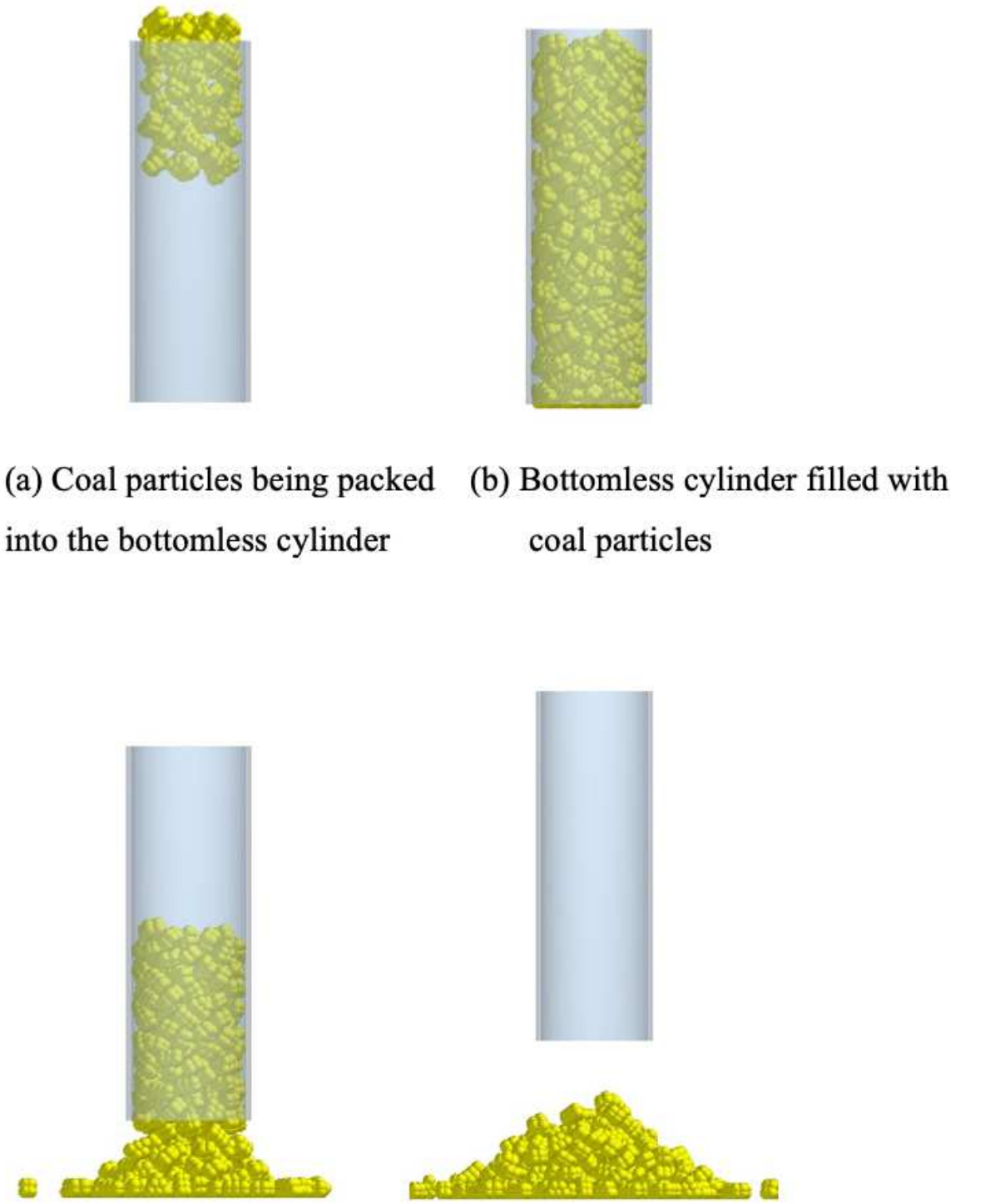

Figure 3

Simulation of the bottomless cylinder test

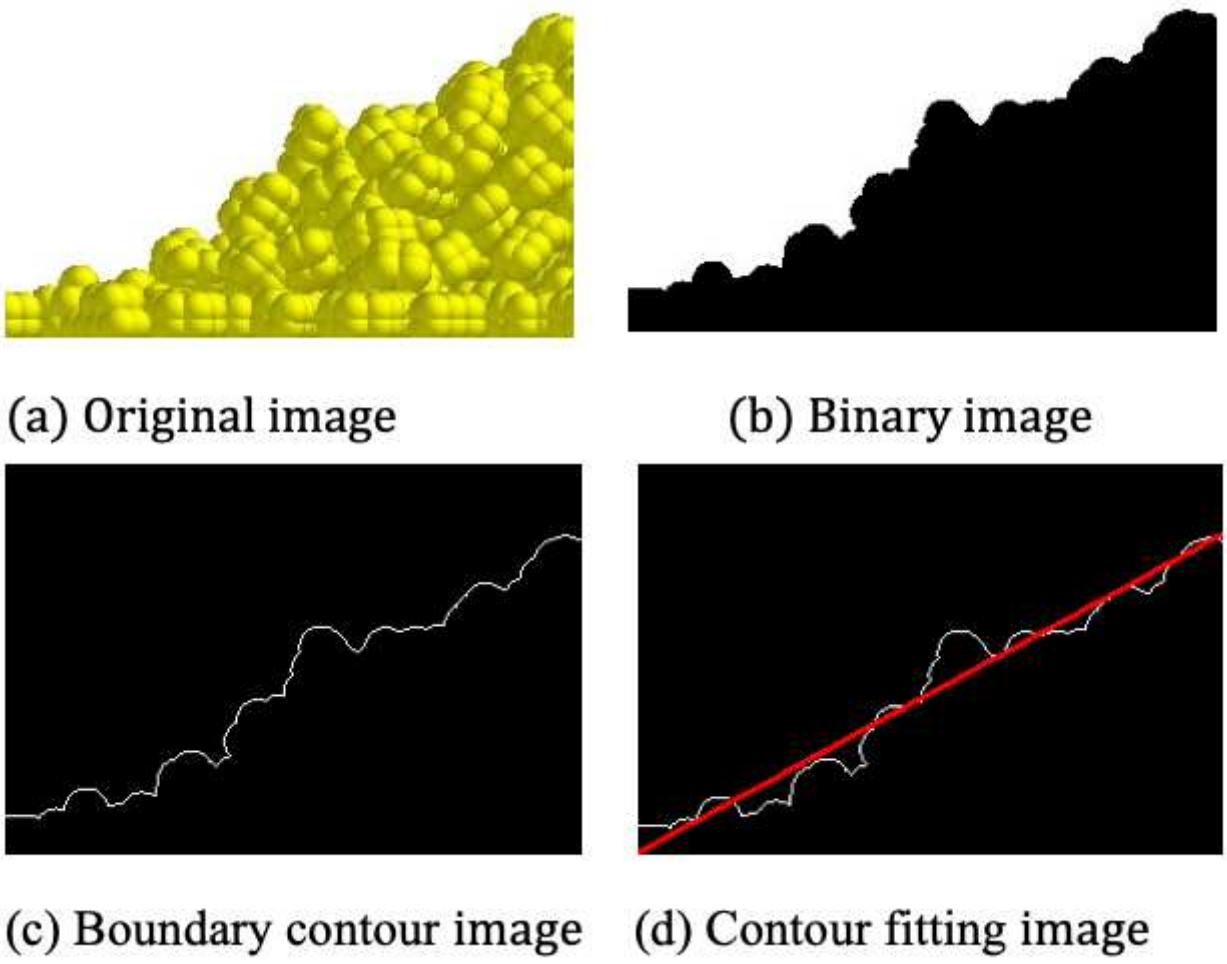

Figure 4

Image processing of the angle of repose measurement

Figure 5

Automatic cylinder testing machine

(a) Actual test

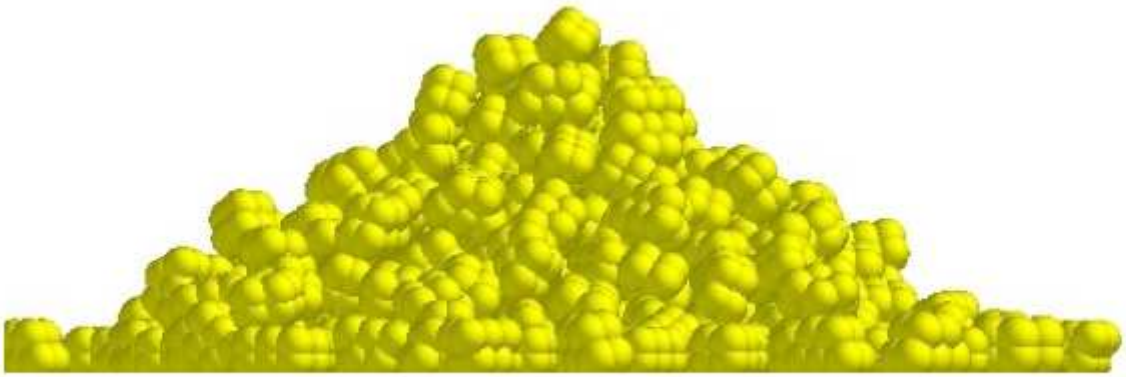

(b) Simulated test

Figure 6

Comparison between actual and simulated tests of coal particle accumulation